Pharmaceutical modulation of canonical Wnt signaling in multipotent stromal cells for improved osteoinductive therapy

Ulf Krause[a,1], Sean Harris[b,1], Angela Green[b], Joni Ylostalo[a], Suzanne Zeitouni[a], Narae Lee[b], and Carl A. Gregory[a,2]

[a]Institute for Regenerative Medicine at Scott and White Hospital, Texas A&M Health Science Center, Temple, TX 76502; and [b]Center for Gene Therapy and Department of Medicine, Tulane University Health Sciences Center, New Orleans, LA 70112

Communicated by Darwin J. Prockop, Texas A&M Health Science Center, Temple, TX, December 16, 2009 (received for review May 20, 2009)

Human mesenchymal stem cells (hMSCs) from bone marrow are regarded as putative osteoblast progenitors in vivo and differentiate into osteoblasts in vitro. Positive signaling by the canonical wingless (Wnt) pathway is critical for the differentiation of MSCs into osteoblasts. In contrast, activation of the peroxisome proliferator-activated receptor-γ (PPARγ)-mediated pathway results in adipogenesis. We therefore compared the effect of glycogen-synthetase-kinase-3β (GSK3β) inhibitors and PPARγ inhibitors on osteogenesis by hMSCs. Both compounds altered the intracellular distribution of β-catenin and GSK3β in a manner consistent with activation of Wnt signaling. With osteogenic supplements, the GSK3β inhibitor 6-bromo-indirubin-3′-oxime (BIO) and the PPARγ inhibitor GW9662 (GW) enhanced early osteogenic markers, alkaline phosphatase (ALP), and osteoprotegerin (OPG) by hMSCs and transcriptome analysis demonstrated up-regulation of genes encoding bone-related structural proteins. At higher doses of the inhibitors, ALP levels were attenuated, but dexamethasone-induced biomineralization was accelerated. When hMSCs were pretreated with BIO or GW and implanted into experimentally induced nonself healing calvarial defects, GW treatment substantially increased the capacity of the cells to repair the bone lesion, whereas BIO treatment had no significant effect. Further investigation indicated that unlike GW, BIO induced cell cycle inhibition in vitro. Furthermore, we found that GW treatment significantly reduced expression of chemokines that may exacerbate neutrophil- and macrophage-mediated cell rejection. These data suggest that use of PPARγ inhibitors during the preparation of hMSCs may enhance the capacity of the cells for osteogenic cytotherapy, whereas adenine analogs such as BIO can adversely affect the viability of hMSC preparations in vitro and in vivo.

osteogenesis | bone repair | tissue engineering

In vitro and in vivo hMSCs can differentiate into osteoblasts, adipocytes, and chondrocytes (1–6), but they also adopt a stromal role, by providing extracellular matrix components, cytokines, and growth factors for paracrine tissue support (7–9). As the presumptive precursors of osteoblasts, hMSCs and related cell lines provide a convenient cell culture model for the study of osteogenic tissue repair in an experimentally accessible system (10). Early studies, employing cultures of osteogenic progenitors, have yielded a wealth of information describing the molecular events that modulate osteogenic differentiation. A critical finding of these studies is that positive signaling by the canonical wingless (Wnt) pathway is essential for differentiation into osteoblasts (11–13). In the canonical Wnt signaling pathway, secreted Wnt ligands bind to the receptor frizzled (Frz) and the coreceptor lipoprotein-related protein 5 and 6 (LRP-5/6) on the target cell. Activation of Frz recruits the cytoplasmic bridging molecule, disheveled (Dsh), so as to inhibit the action of glycogen synthetase kinase-3β (GSK3β). Inhibition of GSK3β decreases phosphorylation of β-catenin, preventing its degradation by the proteasome. Stabilized β-catenin acts on the nucleus by activating T cell factor/lymphoid enhancing factor mediated transcription of target genes that elicit a variety of effects, including induction of differentiation and, in some cases, proliferation. Canonical Wnt signaling is tightly regulated by a combination of positive induction through the binding of the Wnt ligand and negative regulation through numerous mechanisms including the secreted glycoprotein dickkopf-1 (Dkk-1) (14). The clinical significance of Wnt signaling in osteogenesis has been highlighted by reports that mutations in LRP5 that prevent Dkk-1 binding cause abnormally high bone density (15), and mutations that render LRP5 functionally null cause a form of osteoporosis (16). To date, most of the studies that address the role of Wnt signaling in osteogenesis have been carried out by using the murine system (17–19), and there is evidence that Wnt signaling may have the contrary effect on hMSCs (20). We therefore sought to investigate the role of Wnt signaling and osteogenesis by human MSCs in more detail. We compared an inhibitor of GSK3β that would be predicted to mimic Wnt signaling through direct stabilization of β-catenin [6-bromo-indirubin-3′-oxime (BIO)] and an inhibitor of PPARγ [GW9662 (GW)] that would be predicted to attenuate inhibitory crosstalk from the adipogenic axis and, therefore, also enhance Wnt signaling (21–23). We found that both BIO and GW increased in vitro mineralization, but expression of early osteogenic markers was biphasic, with higher doses becoming inhibitory. When implanted into mice harboring calvarial defects, hMSCs pretreated with GW substantially accelerated healing, whereas those pretreated with BIO had no effect. Further investigation indicated that unlike GW, BIO attenuated hMSC renewal in vitro. Furthermore, we found that GW treatment significantly reduced expression of chemokines that may exacerbate neutrophil- and macrophage-mediated cell rejection. These data suggest that use of PPARγ inhibitors during the preparation of hMSCs substantially and reliably enhances the capacity of hMSCs for osteogenic cytotherapy, whereas adenine analogs such as BIO have complicated and unpredictable effects on viability and efficacy.

Results

Effect of Dkk-1 and PPARγ Agonists on the Expression of ALP. To confirm that Wnt signaling is necessary for the differentiation of hMSCs into osteoblasts, we incubated MSCs in osteoinductive media containing no dexamethasone (dex) for 8 days and measured activity of alkaline phosphatase (ALP). Although it is conventional to add dexamethasone for osteogenesis, given its powerful pleiotropic effects and the observation that early osteogenic markers such as ALP can be activated without its presence (Fig. S1*A*), initial experiments were performed in the absence of dexamethasone. When the Wnt inhibitor Dkk-1 was added to block canonical Wnt

Author contributions: U.K. and C.A.G. designed research; U.K., S.H., A.G., J.Y., S.Z., N.L., and C.A.G. performed research; U.K., J.Y., and C.A.G. analyzed data; and U.K. and C.A.G. wrote the paper.

The authors declare no conflict of interest.

[1]U.K. and S.H. contributed equally to the work.

[2]To whom correspondence should be addressed. E-mail: cgregory@medicine.tamhsc.edu.

This article contains supporting information online at www.pnas.org/cgi/content/full/0914360107/DCSupplemental.

signaling, ALP activity was attenuated (Fig. 1*A*). We then examined PPARγ activity on osteogenesis because the PPARγ activity enhances adipogenesis while inhibiting the Wnt-mediated osteogenic axis of differentiation (20, 21). ALP function was dose-dependently down-regulated upon incubation with troglitazone and also other synthetic PPARγ agonists (Fig. 1*B* and Fig. S1).

Effect of GSK3β and PPARγ Inhibition on Intracellular Redistribution of GSK3β and β-Catenin. We examined whether inhibition of GSK3β would mimic Wnt signaling through direct stabilization of β-catenin, and whether inhibition of PPARγ would blunt inhibitory crosstalk from the adipogenic axis, therefore also resulting in enhancement of Wnt signaling (Fig. 2*A*) (21–23). The inhibitors BIO and GW were chosen because of their specificity for GSK3β and PPARγ, respectively (Fig. 2*A*). Incubation of both inhibitors with MSCs under osteogenic conditions resulted in increased levels of nuclear β-catenin (Fig. 2 *B* and *C*) and depletion of GSK3β from the cytoplasm (Fig. 2*D*). Interestingly, cytosolic depletion of GSK3β occurred, even though the proposed mechanism of BIO or GW does not predict up-regulation of a Wnt/Frz/LRP/Dsh receptor complex. It is currently unclear whether GSK3β is degraded or relocalized upon treatment with BIO/GW. Nonetheless, both nuclear localization of β-catenin and depletion of cytosolic GSK3β are consistent with enhancement of canonical Wnt signaling. Furthermore, incubation of hMSCs in either BIO or GW reduced nuclear levels of PPARγ, also suggesting that the canonical Wnt axis was predominating in the treated cells.

Effect of GSK3β and PPARγ Inhibition on the Expression of ALP, OPG, and Dkk-1. To examine whether the up-regulation of Wnt signaling by the inhibitors affected early stage osteogenesis by MSCs, they were incubated in osteogenic medium lacking dex but containing BIO or GW. After 8 days of culture, ALP activity and the secretion of OPG were measured. Both inhibitors induced the ALP activity, but this was observed at low doses of inhibitor; in the case of BIO, the maximal effect was observed between 100 and 200 nM and for GW, the effect occurred at doses between 0.5 and 1.0 μM. At higher doses, exceeding 400 nM BIO or 1.0 μM GW, ALP activity dropped back to control levels (Fig. 3*A*). Secretion of OPG rose in a dose-dependent manner upon incubation with BIO, but reached maximal stimulation at 0.5 μM GW (Fig. 3*B*). It has been speculated that arrest of canonical Wnt signaling occurs during terminal differentiation of osteoprogenitor cells, and Dkk-1 has been implicated in this process (24, 25). Dkk-1 secretion was reduced in all cases, with maximal inhibition occurring at concentrations that induced highest ALP activity (Fig. 3*C*). Even though Dkk-1 levels were slightly elevated with higher GW and BIO doses, they remained significantly lower than the control. A substantial reduction of hMSC yield was evident when exposed to concentrations >400 nM BIO. This effect did not seem to arise from canonical Wnt signaling

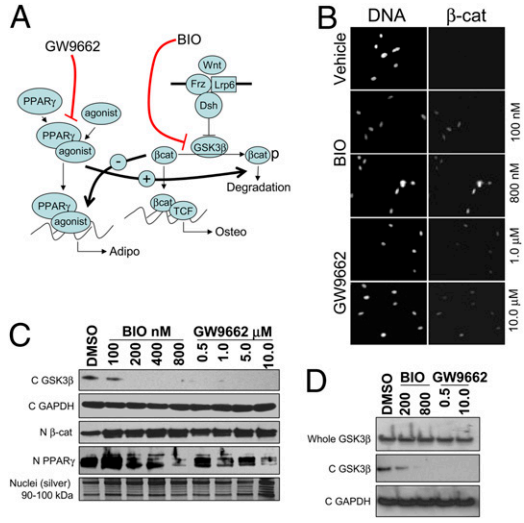

Fig. 2. In vitro effects of GW9662 and BIO on Wnt signaling in hMSCs. (*A*) BIO and GW are predicted to up-regulate Wnt signaling by direct inhibition of GSK3β or by ablating PPARγ-mediated negative crosstalk, respectively. (*B*) Fluorescent microscopy of hMSCs with counterstained nuclei (pico-green; *Left*) or cy-3 labeled anti-β-catenin stained nuclei (*Right*) (*C*) Immunoblots of cytosolic GSK3β (C GSK3β), nuclear β-catenin (N β-cat), and nuclear PPARγ (N –PPARγ) on extracts of hMSCs treated with BIO or GW. Blots were normalized for cytosolic proteins with GAPDH (C GAPDH) and for nuclear proteins by silver stain. (*D*) Immunoblots of whole cell and cytosolic extracts of hMSCs.

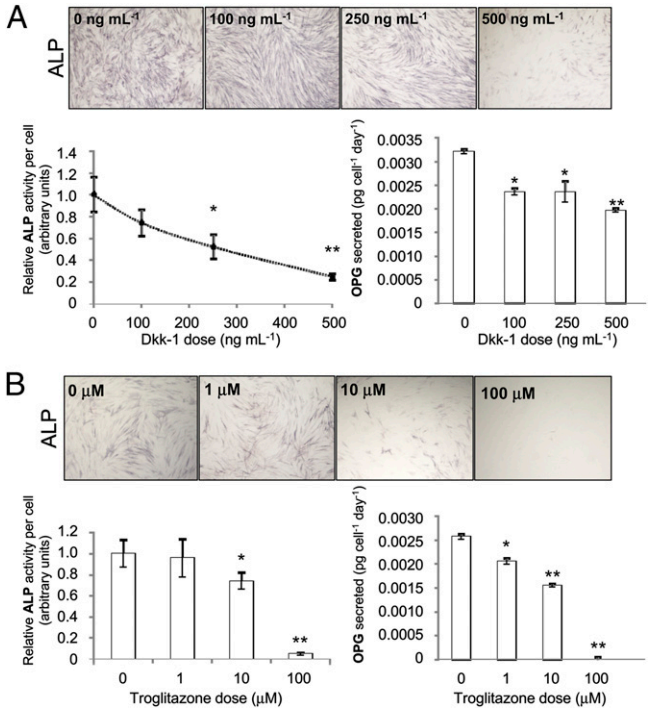

Fig. 1. Effect of Dkk-1 (*A*) or the PPARγ agonist, troglitazone (*B*), on ALP activity and OPG secretion. ALP activity was visualized by staining and measured by colorimetric assay. OPG was measured from the medium by ELISA. Values were normalized to cell number. Data are means ± SD ($n = 6$); *, $P < 0.05$, **, $P < 0.01$.

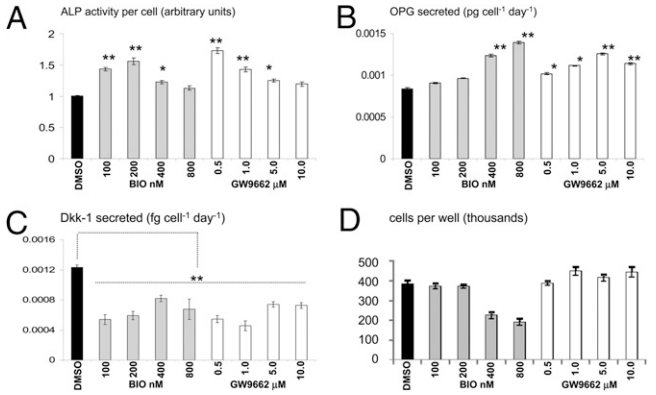

Fig. 3. hMSCs were incubated in osteogenic media with BIO or GW. After 8 days of culture, ALP activity was measured (*A*) and normalized to cell number (*D*). OPG and Dkk-1 was measured from the media by ELISA (*B* and *C*). Data are means ± SD ($n = 6$); *, $P < 0.05$, **, $P < 0.01$.

because GW elicited the same effects on β-catenin, GSK3β redistribution, and stimulation of early osteogenic markers without reduction in cellular yield. Although BIO is highly specific for GSK3β (26), the parent molecule, indirubin monooxime has been shown to inhibit cyclin dependent kinases at high concentrations (27). Cell cycle analysis demonstrated that hMSCs treated with 800 nM BIO exhibited a similar DNA profile to those that are heavily contact inhibited, suggesting that high doses of BIO inhibit mitosis (Fig. S2*A*). The absence of apoptotic morphology, a pre-G1 peak, and no detectable levels of cleaved caspase 3 (Fig. S2*B*) confirmed apoptosis was also not responsible for the reduced cell yield.

Effects of GSK3β and PPARγ Inhibition on the Transcriptome of hMSCs. Inhibition of GSK3β and PPARγ appeared to increase the level of Wnt signaling concomitantly with increased OPG secretion and ALP activity. These observations suggested that the inhibitors had enhanced the early stages of osteogenesis through acceleration of canonical Wnt signaling at the expense of PPARγ activity. To examine this phenomenon in more detail, hMSCs were incubated in osteogenic media lacking dex, but containing high (800 nM BIO and 10 μM GW) and low (200 nM BIO and 1.0 μM GW) doses of the inhibitors. After 8 days of culture, RNA microarrays were performed on the hMSCs. Initial inspection of the datasets demonstrated that they shared similarities with a similar study involving human fibroblasts and Wnt3a, suggesting that canonical Wnt signaling had been accelerated (Table S1). Irrespective of dose, differentially transcribed genes clustered into two general groups with strong statistical significance ($P < 0.0001$ for all cases, Fig. S3)—(*i*) up-regulated in GW- and BIO-treated cells compared to the vehicle control and (*ii*) up-regulated in the vehicle control compared to BIO and GW. Gene clusters were sorted into gene ontology (GO) tags based on known function. The majority of GO tags in cluster I (Table S2) consisted of membrane, mRNA processing, and intracellular rearrangement-related functions as well as collagen and extracellular matrix (ECM) groups. The Wnt/β-catenin GO group was also significantly represented in this cluster. Upon examination of individual fold-changes for differentially expressed ECM genes, it was evident that collagens and ECM proteins found in bone tissue were up-regulated, whereas those found in other tissues were reduced or unchanged (Table S3). Of interest was the down-regulation of matrix metalloproteinase I, matrix gla-protein and oncostatin M, all associated with inhibition of osteogenesis or bone catabolism. Cluster II consisted mainly of genes responsible for steroid and lipid processing (Table S4). Of note was the prevalence of prostaglandin and lipid modifying enzymes in this cluster because these processes often provide ligands for PPARγ (28) as well as enrichment of sphingomyelin- and ceramide-related genes, which are strongly associated with lipid and steroid homeostasis (29, 30).

Effect of GSK3β and PPARγ Inhibition on Late Stage Osteogenesis. Extended periods of incubation in BIO and GW in the absence of dex did not induce biomineralization, so we therefore measured the effect of the inhibitors in its presence. Initially, we examined whether pretreatment of hMSCs with inhibitors BIO (200 and 800nM) and GW (1.0 and 10.0 μM) in the presence of β-glycerophosphate (β-GP) and ascorbate for 8 days, followed by 15 days in the same media supplemented with dex, affected mineralization of the cultures. If BIO or GW function to accelerate the cells through the immature stages of osteogenesis and partially to maturity, hMSCs exposed to these conditions would be expected to respond more rapidly to the steroid-dependent mature osteoblast transition. After differentiation, calcium content was visualized by Alizarin Red S (ARS) staining, and the dye was extracted and quantified. At the doses tested, and in a dose-dependent manner, BIO and GW enhanced dex-induced differentiation into biomineralizing osteoblasts (Fig. 4).

We then examined whether withdrawal of the Wnt stimulus caused by BIO and GW was necessary for the hMSCs to progress to a dex-dependent biomineralizing phenotype. Human MSCs were precultured with BIO and GW in the presence of β-GP, ascorbate, and dex for 17 days. Once again, inhibitor treatment enhanced dex-induced biomineralization (Fig. 5), suggesting that the action of BIO and GW enhances the early stages of osteogenesis and removal of the stimulus is not required to complete the process. Data from both experiments suggest that Wnt modulation is necessary to induce an early osteoprogenitor-like phenotype in hMSCs, and this process can occur simultaneously with terminal differentiation.

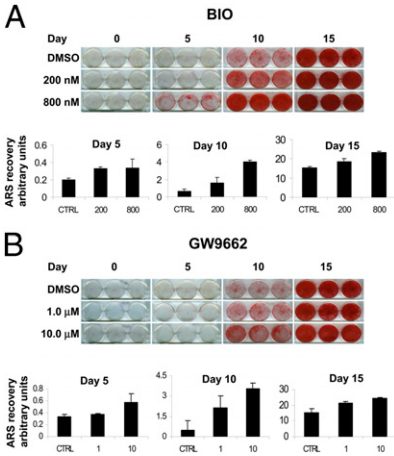

Fig. 4. MSCs were incubated in osteogenic media containing BIO or GW for 8 days. The cultures then received dex containing osteogenic media for a further 15 days (Fig. S6*A*). Cultures were stained for calcium with ARS. For semiquantification, the stain was re-extracted and measured spectrophotometrically. Both BIO (*A*) and GW (*B*) pretreatment enhanced mineralization.

Clotted Human Plasma Is a Biocompatible and Osteoinductive Vector for Administration of hMSCs. In anticipation of in vivo experiments testing the potential efficacy of the inhibitor treated hMSCs for the repair of bone, we examined a number of matrices for cell administration. We found that clotted human plasma sustained the survival and proliferation of hMSCs in vitro and also accelerated steroid-induced biomineralization. When monolayers of hMSCs are partially covered with a meniscus of clotted human plasma, the cells in contact with the plasma mineralize faster than the uncovered portion of the monolayer when dex-containing osteogenic media is provided (Fig. S4).

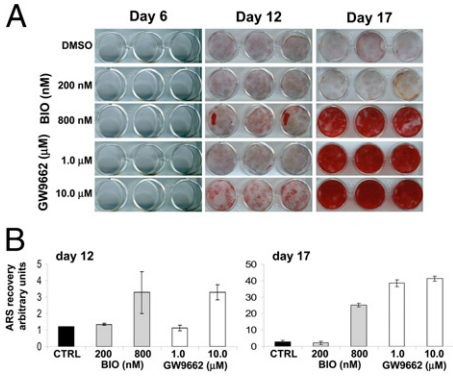

Fig. 5. Cultures were incubated in osteogenic media containing dex and BIO or GW (Fig. S6*B*). After 17 days, monolayers were stained for calcium with ARS (*A*). For semiquantification, the stain was re-extracted and measured spectrophotometrically (*B*).

Effects of GSK3β and PPARγ Inhibition on Repair of an Experimental Induced Cranial Defect in Mice. Given that BIO and GW accelerated osteogenic differentiation by human MSCs *in vitro*, we tested whether the treated hMSCs could repair a critical bone defect *in vivo*. Human MSCs were cultured in the presence of osteogenic medium lacking dex, but containing BIO (200 and 800 nM) or GW (1.0 and 10.0 μM). Calvarial lesions were generated in nude mice and 1×10^6 hMSCs, mixed with human plasma, were applied, followed by thromboplastin to initiate gelling. The scalp was sutured, and the animals were allowed to heal. Initially, short-duration experiments were performed to monitor distribution of the hMSCs and to ensure the cells had survived the implantation process. GFP-labeled hMSCs were administered, and mice were killed after 24 h. Upon histological analysis, a substantial number of GFP-labeled, healthy hMSCs had formed a thick layer over the injury and adjacent bone tissue (Fig. S5 *A* and *B*). The hMSCs could be readily detected with an antibody for membrane localized human β-2 microglobulin (Fig. S5 *C* and *D*). Robust antibody detection of unmanipulated hMSCs, rather than lentiviral labeling, was favored in long-term experiments because very low passage hMSCs could be used, rather than genetically tagged preparations that had undergone a number of passages. Long-term experiments were performed for 50 days, with additional doses of hMSCs administered at day 14, 28, and 42 by direct injection of a plasma:hMSC mixture under the scalp (Fig. 6*A*). At day 50, the crania were explanted and x-ray images of the calvarial lesions were taken. The digitized images were then analyzed densitometrically to quantify the degree of bone accrual (Fig. 6*B*). The lesioned side was compared with the contralateral side, and data were expressed as the ratio of radio-opacity on the lesioned side to the contralateral side. Surprisingly, GW, but not BIO, significantly improved the ability of MSCs to repair cranial lesions when compared to MSCs that were not drug treated. Upon histological analysis, new bone formation was detected in the GW groups, and in the case of the 10 μM GW group, marrow sinusoids were evident in the newly formed bone (Fig. 7*A*), which could be identified by tetracycline incorporation (Fig. 7*B*). In contrast, there was no significant sign of bone repair in the mock groups that received plasma alone, and control hMSC groups that received cells

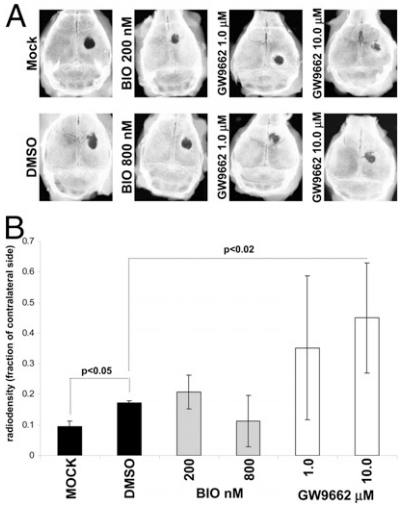

Fig. 6. Three-millimeter-diameter calvarial defects were induced in nude mice. One million hMSCs pretreated with BIO or GW were mixed with plasma and administered to the bone lesion. Subsequent doses were injected at 14-day intervals until day 50 (Fig. S6*C*). (*A*) X-rays of explanted crania. For the GW group, specimens representing the range of the standard deviations are presented. (*B*) The ratio of lesioned to contralateral (intact side) radio-opacity calculated by image analysis software. Data are means ± SD (n = 6, n = 5 for mock).

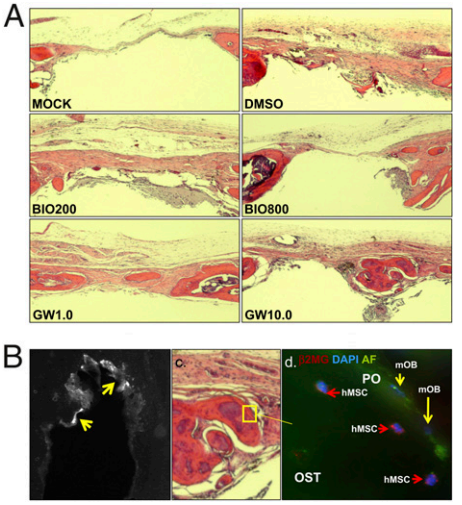

Fig. 7. (*A*) Hematoxylin and eosin-stained longitudinal sections at the diameter of the lesions. New bone can be seen in the GW-treated injuries. (*B*) UV microscopy of transverse sections for tetracycline (new bone) deposition (arrowed). (*C*) Immuno-histochemical staining of hMSCs embedded in new bone of the GW-treated calvaria. Unstained murine osteoblasts (mOB) are also visible. OST, osteoid; PO, periosteum.

treated with DMSO or BIO. When the sections were stained with anti-β-2 microglobulin, isolated clusters of hMSCs from only control and GW groups were detected (Fig. 7 *C* and *D*). However, no more than a few hundred cells could be counted throughout the entire lesion, suggesting that the majority of cells had either died or migrated away. In both control groups and in the GW-treated groups, we detected blood vessels, demonstrating that GW treatment had not affected the ability of MSCs to initiate angiogenesis at trauma sites (Fig. 8*A*).

Enhanced compatibility of the GW-treated hMSCs for the osteogenic niche could explain the increased efficacy, but not the failure of the BIO-treated cells. However, upon further inspection of the microarray data, a minor cluster was identified where genes were profoundly down-regulated in GW-treated MSCs, and notably up-regulated in BIO-treated MSCs as compared to the control. This cluster was highly enriched for inflammatory mediators, including IL-1, IL-8, and inflammatory chemokines of the CXC family (Table S5). These data could be validated in most cases by ELISA analysis of supernates from treated hMSC cultures (Tables S6 and S7). Because nude mice are able to elicit a macrophage- and neutrophil-mediated response, it is probable that the GW-treated MSCs were protected by reduced expression of chemoattractants. Furthermore, because we could not detect new bone, hMSCs, or blood vessels in the BIO-hMSC treated calvaria, it is likely that a combination of decreased viability and cell-mediated rejection rendered these cells inactive.

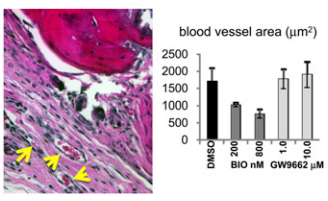

Fig. 8. Blood vessels were identified on hematoxylin and eosin-stained sections (*A*, arrowed) corresponding to 0.5 mm either side of the diameter of the lesion. (*B*) Six-micrometer sections were surveyed every 30 μm, and blood vessel area was calculated. Data are means ± SD (n = 3 animals).

Discussion

Cultures of hMSCs are inherently heterogeneous, with the individuals of the population possessing different propensities for osteogenesis, chondrogenesis, adipogenesis, or proliferation. Heterogeneity can arise from the nature of the donor, the number of past cell doublings, and cell density. Evidence suggests that the history of a given hMSC, with respect to the number of cell doublings, and past exposure to different levels of cell density, in most cases can affect the propensity of a given cell to divide or differentiate (31–33). This apparently stochastic distribution of cellular characteristics can be controlled in part by the addition of cytokines, growth factors, and/or drugs. Given that both Wnt signaling and blunting of the adipogenic axis are necessary for the initiation of osteogenic processes in MSCs, we sought to investigate the role of small molecule inhibitors in controlling the events. We found that Wnt signaling could be increased in MSCs by either direct inhbition of GSK3β or by inhibiting the master regulator of adipogenesis, PPARγ. These observations supported the widespread notion that negative crosstalk occurs between the canonical Wnt and PPARγ axis. At lower doses, we could significantly enhance the expression of early osteogenic markers in hMSCs by treatment with either inhibitor, but osteogenic enhancement was attenuated at higher doses. In contrast, when hMSCs were pretreated or simultaneously treated with BIO or GW, and subjected to dex-dependent osteogenesis, mineralization was up-regulated in a dose-dependent manner. A simple interpretation of these results leads to the conclusion that endogenous canonical Wnt signaling can enhance osteogenesis. However, in light of an elegant series of experiments carried out by Liu et al. (25), the mechanism seems more complex. In this instance, canonical Wnts1 and 3a could inhibit ALP and mineralization by hMSCs at high concentrations; however, when hMSCs were subjected to a bimodal culture system where adipogenic and osteogenic supplements were available, canonical Wnt signaling tipped the balance in favor of osteogenesis. It is possible, therefore, the high-serum culture system used in our experiments reflects a similar situation, with modest osteogenic and adipogenic stimuli affecting a balanced steady state on the cells. The presence of GW and BIO, therefore, disrupts the balance of the culture in favor of the osteogenic lineage. In contrast, high concentrations of PPARγ agonists in our osteogenic cultures containing dex initiate adipogenesis rather than osteogenesis (Fig. S1*C*).

When implanted into experimentally induced calvarial defects in mice, GW-treated hMSCs profoundly improved healing and induced angiogenesis. Although vehicle-treated hMSCs could not significantly enhance bone repair, angiogenesis was also induced, suggesting that even vehicle-treated hMSCs had survived at the site for a duration sufficient to initiate the process. Because BIO-treated cells had neither an effect on bone repair or angiogenesis, and could not be detected directly, it appeared that the cells rapidly died upon administration or migrated from the site. Given the effects of BIO on hMSCs in vitro, the former is most probable. Although the efficacy of GW-treated hMSCs is probably due to enhanced osteogenic propensity and angiogenic properties, substantial down-regulation of immune chemokines is also likely to extend their survival. Nevertheless, even the in vivo survival of GW-treated hMSCs was transient, suggesting a support role for hMSCs where the cells transiently up-regulate angiogenesis and inherent osteogenic capacity of the host's tissue. In agreement with this observation, it has recently been demonstrated that a population of hMSCs with an enhanced endogenous canonical Wnt signaling serves to enhance synergistically the ostoegenic capacity of coadministered hMSCs with a lesser degree of Wnt signaling (25).

Pharmaceutical modulation of canonical Wnt signaling can increase the osteogenic capacity of hMSCs, but the small molecules necessary for such a task have a broad spectrum of side effects that may preclude the cells' efficacy in vivo. Nevertheless, we found that hMSCs treated with GW, an inhibitor of PPARγ, had increased their osteogenic propensity without blunting viability or their ability to perform ancillary tasks such as angiogenic stimulation. The modified cultures are essentially a combination of stromal stem cells and osteoblasts, with properties of both. Therefore, hMSCs prepared in this manner are a unique and rationally designed cytotherapeutic with profoundly enhanced efficacy for bone repair.

Experimental Procedures

For additional detail, refer to *SI Experimental Procedures*.

Tissue Culture. Iliac crest bone marrow aspirates (2 mL) were drawn in accordance with institutional review board approval. Mesenchymal stem cells were prepared from the mononuclear fraction of the aspirates as described (31, 34).

Early Osteogenic Differentiation and Alkaline Phosphatase Assays. MSCs were plated in six-well plates at an initial plating density of 100 cells/cm^2 and cultured in standard complete media for 6 days until semiconfluence (≈5,000 cells per cm^2). Osteogenic base media consisting of complete media containing 5 mg·mL^{-1} β-GP and 50 μg·mL^{-1} ascorbate-2-phosphate (Sigma, Poole, Dorset, UK), and the appropriate inhibitor or vehicle was then used to induce early osteogenic differentiation. Assays were allowed to proceed for 8–10 days with changes of media every 2 days. ALP assays were performed as described (35).

Cell Cycle. Profiles were generated by fluorescence-activated cell sorting (Beckman Coulter FC500) and analyzed with MultiCycleAV (Phoenix Flow Systems) software.

Array Analysis. Transcriptome arrays were performed by using Affymetrix apparatus and HG-U133 Plus 2.0 chips. Cytokine arrays on conditioned media were performed by using a human cytokine array (RayBiotech) and analyzed by using a digital imager (Versadoc; Bio-Rad, Hercules, CA).

ELISAs. Assays for Dkk-1 and OPG were carried out by using nonbiotinylated polyclonal capture antibodies and biotinylated detection antibodies that were commercially acquired (R&D Systems, Minneapolis) on Nunc Immunosorp coated 96-well plates (Fisher Lifesciences, Pittsburgh). The biotinylated capture antibodies were detected by using horseradish peroxidase-conjugated streptavidin and TMB substrate (Pierce, Rockford, IL).

Protein Extraction, Gel Electrophoresis, and Western Blotting. Nuclear extracts were performed by Triton extraction and differential centrifugation as described (36). Proteins were electrophoresed and blotted onto nitrocellulose by using the Novex electrophoresis system (Invitrogen, Carlsbad, CA).

Late-Stage Osteogenesis and ARS Staining. Mature osteogenic assays were performed in six-well format as described (10).

Clotted Plasma Coculture. Confluent monolayers of MSCs were generated in wells of a 12-well tissue culture plate. Human plasma was added to each well so as to cover ≈30% of the surface area. After the plasma had clotted, osteogenic assays were then performed by using standard media preparations.

Calvarial Lesions. MSCs were cultured in the presence of osteogenic base media containing the appropriate inhibitor or vehicle. After 8 days, they were suspended in human plasma and administered to nude mice that had received a circular lesion in the cranium. Subsequent doses of cells were administered by direct injection in plasma/thromboplastin mix.

X-ray Imaging and Quantification. Cranial bones were imaged by x-ray under anesthesia (Faxitron M20). Digital images were be captured on a digital plate and processed on a phosphorimager

reader (PMI; Bio-Rad) and processed by volume analysis software (Quantity One; Bio-Rad).

Histochemistry and Immunocytochemistry. For β-catenin localization studies, hMSCs were stained with a cy-3 conjugated anti-β-catenin antibody (clone 15B8; Sigma, St. Louis), and nuclei were counterstained with pico-green dye (Invitrogen). Specimens were processed as paraffin blocks and 8-μm longitudinal sections were prepared, deparaffinized, and rehydrated, then stained with hematoxylin and eosin (Sigma). For immunocytochemistry, sections were probed with an anti-human β-2-microglobulin antibody. An upright fluorescent microscope (Eclipse H600L; Nikon) fitted with a high performance camera (Retiga 2000R) and image analysis software (NiSElements; Nikon) was employed for imaging.

Tetracycline Tracing of in Vivo Calcium Deposition. The tetracycline was imaged by using an upright fluorescent microscope (Eclipse H600L; Nikon) fitted with a high performance camera (Retiga 2000R) and analyzed by using NiSElements software (Nikon). Embedding, sectioning, and mounting were carried out on nondecalcified material.

Semiquantitative Blood Vessel Measurements. Calvaria were fixed, decalcified and sectioned in paraffin, and stained with hematoxylin and eosin as described. Using NIS-Elements image analysis software, the surface area of blood vessels in a defined region of interest was calculated and totaled (*SI Experimental Procedures*). The values were expressed as the mean of total blood vessel area from three animals per group.

ACKNOWLEDGMENTS. We thank Kent Claypool, Institute for Regenerative Medicine, Texas A&M Health Sciences Center, for assistance with flow cytometry and Jack Ratcliff (Franklin, TN) for processing calcified bone specimens. This work was supported in part by National Institutes of Health Grants HL075161-01, DK071780, and R020152, the Louisiana Gene Therapy Research Consortium, Scott and White Hospital, and Texas A&M Health Sciences Center.

1. Friedenstein A-J, Gorskaja JF, Kulagina NN (1976) Fibroblast precursors in normal and irradiated mouse hematopoietic organs. *Exp Hematol* 4:267–274.
2. Friedenstein A-J, Chailakhyan R-K, Gerasimov U-V (1987) Bone marrow osteogenic stem cells: *in vitro* cultivation and transplantation in diffusion chambers. *Cell Tissue Kinet* 20:263–272.
3. Pereira R-F, et al. (1995) Cultured adherent cells from marrow can serve as long-lasting precursor cells for bone, cartilage, and lung in irradiated mice. *Proc Natl Acad Sci USA* 92:4857–4861.
4. Pittenger M-F, et al. (1999) Multilineage potential of adult hMSCs. *Science* 284: 143–147.
5. Sekiya I, Vuoristo J-T, Larson B-L, Prockop D-J (2002) In vitro cartilage formation by human adult stem cells from bone marrow stroma defines the sequence of cellular and molecular events during chondrogenesis. *Proc Natl Acad Sci USA* 99:4397–4402.
6. Sekiya I, Larson B-L, Vuoristo J-T, Cui J-G, Prockop D-J (2004) Adipogenic differentiation of human adult stem cells from bone marrow stroma (MSCs). *J Bone Miner Res* 19: 256–264.
7. Dexter TM, Spooncer E, Schofield R, Lord BI, Simmons P (1984) Haemopoietic stem cells and the problem of self-renewal. *Blood Cells* 10:315–339.
8. Austin TW, Solar GP, Ziegler FC, Liem L, Matthews W (1997) A role for the Wnt gene family in hematopoiesis: expansion of multilineage progenitor cells. *Blood* 89: 3624–3635.
9. Van Den Berg D-J, Sharma A-K, Bruno E, Hoffman R (1998) Role of members of the Wnt gene family in human hematopoiesis. *Blood* 92:3189–3202.
10. Gregory C-A, Gunn W-G, Peister A, Prockop D-J (2004) An Alizarin red-based assay of mineralization by adherent cells in culture: comparison with cetylpyridinium chloride extraction. *Anal Biochem* 329:77–84.
11. Bain G, Müller T, Wang X, Papkoff J (2003) Activated beta-catenin induces osteoblast differentiation of C3H10T1/2 cells and participates in BMP2 mediated signal transduction. *Biochem Biophys Res Commun* 301:84–91.
12. Rawadi G, Vayssière B, Dunn F, Baron R, Roman-Roman S (2003) BMP-2 controls alkaline phosphatase expression and osteoblast mineralization by a Wnt autocrine loop. *J Bone Miner Res* 18:1842–1853.
13. Gregory C-A, Green A, Lee N, Rao A, Gunn W (2006) The promise of canonical Wnt signaling modulators in enhancing bone repair. *Drug News Perspect* 19:445–452.
14. Tian E, et al. (2003) The role of the Wnt-signaling antagonist DKK1 in the development of osteolytic lesions in multiple myeloma. *N Engl J Med* 349:2483–2494.
15. Boyden L-M, et al. (2002) High bone density due to a mutation in LRP5. *N Engl J Med* 346:1513–1521.
16. Gong Y, et al; Osteoporosis-Pseudoglioma Syndrome Collaborative Group (2001) LDL receptor-related protein 5 (LRP5) affects bone accrual and eye development. *Cell* 107: 513–523.
17. Bennett C-N, et al. (2005) Regulation of osteoblastogenesis and bone mass by Wnt10b. *Proc Natl Acad Sci USA* 102:3324–3329.
18. Clément-Lacroix P, et al. (2006) Lrp5-independent activation of Wnt signaling by lithium chloride increases bone formation and bone mass in mice. *Proc Natl Acad Sci USA* 102: 17406–17411.
19. Kulkarni N-H, et al. (2006) Orally bioavailable GSK-3α/β dual inhibitor increases markers of cellular differentiation in vitro and bone mass *in vivo*. *J Bone Miner Res* 21:910–920.
20. Boland G-M, Perkins G, Hall D-J, Tuan R-S (2004) Wnt 3a promotes proliferation and suppresses osteogenic differentiation of adult human MSCs. *J Cell Biochem* 93: 1210–1230.
21. Farmer S-R (2005) Regulation of PPARγ activity during adipogenesis. *Int J Obes (Lond)* 29:13–16.
22. Akune T, et al. (2004) PPARgamma insufficiency enhances osteogenesis through osteoblast formation from bone marrow progenitors. *J Clin Invest* 113:846–855.
23. Liu J, Farmer S-R (2004) Regulating the balance between PPARγ and β-catenin signaling during adipogenesis. A GSK3β phosphorylation-defective mutant of β-catenin inhibits expression of a subset of adipogenic genes. *J Biol Chem* 279:45020–45027.
24. van der Horst G, et al. (2005) Downregulation of Wnt signaling by increased expression of Dickkopf-1 and -2 is a prerequisite for late-stage osteoblast differentiation of KS483 cells. *J Bone Miner Res* 20:1867–1877.
25. Liu G, et al. (2009) Canonical Wnts function as potent regulators of osteogenesis by human MSCs. *J Cell Biol* 185:67–75.
26. Meijer L, et al. (2003) GSK-3-selective inhibitors derived from Tyrian purple indirubins. *Chem Biol* 10:1255–1266.
27. Damiens E, Baratte B, Marie D, Eisenbrand G, Meijer L (2001) Anti-mitotic properties of indirubin-3′-monoxime, a CDK/GSK-3 inhibitor: induction of endoreplication following prophase arrest. *Oncogene* 20:3786–3797.
28. Kota B-P, Huang T-H, Roufogalis B-D (2005) An overview on biological mechanisms of PPARs. *Pharmacol Res* 51:85–94.
29. Lucki N-C, Sewer M-B (2008) Multiple roles for sphingolipids in steroid hormone biosynthesis. *Subcell Biochem* 49:387–412.
30. Worgall T-S (2008) Regulation of lipid metabolism by sphingolipids. *Subcell Biochem* 49:371–385.
31. Sekiya I, et al. (2002) Expansion of human adult stem cells from bone marrow stroma: Conditions that maximize the yields of early progenitors and evaluate their quality. *Stem Cells* 20:530–541.
32. Gregory C-A, Ylostalo J, Prockop D-J (2005) Adult bone marrow stem/progenitor cells (MSCs) are pre-conditioned by micro-environmental "niches" in culture. *Sci STKE* 294: pe37.
33. Larson BL, Ylöstalo J, Prockop DJ (2008) Human multipotent stromal cells undergo sharp transition from division to development in culture. *Stem Cells* 26:193–201.
34. Colter D-C, Class R, DiGirolamo C-M, Prockop D-J (2000) Rapid expansion of recycling stem cells in cultures of plastic-adherent cells from human bone marrow. *Proc Natl Acad Sci USA* 97:3213–3218.
35. Gunn W-G, et al. (2005) A crosstalk between myeloma cells and MSCs stimulates production of DKK1 and IL-6. *Stem Cells* 24:986–991.
36. Gregory C-A, Singh H, Perry A-S, Prockop D-J (2003) Wnt signaling inhibitor Dkk-1 is required for re-entry into the cell cycle of hMSCs. *J Biol Chem* 278:28067–28078.